DEVELOPMENT OF ANNULAR COUPLED STRUCTURE

T. Kageyama, Y. Morozumi, K. Yoshino and Y. Yamazaki
KEK, National Laboratory for High Energy Physics
Oho 1-1, Tsukuba-shi, Ibaraki-ken 305, Japan

Abstract

This paper summarizes the development of a $\pi/2$-mode standing-wave Annular Coupled Structure (f=1.296GHz) for the JHP (Japanese Hadron Project) 1-GeV proton linac. This ACS has four coupling slots between the accelerating and annular coupling cells to suppress higher order mode mixing with the coupling mode. To demonstrate the feasibility of the four-slot ACS, high-β (β=v/c=0.78) and low-β (0.52) prototype cavities have been constructed and successfully tested up to each design RF power. Concerning the field distortion due to the coupling slots, the four-slot ACS gives an almost axially symmetric accelerating field. At present, subsequent R&D work on production model cavities is underway.

Introduction

In an ACS cavity operated in the $\pi/2$ standing-wave mode [1], accelerating cells and non-excited annular coupling cells are alternately located as shown in Fig. 1. It is the annular coupling cell that features the RF properties of the ACS. An annular cavity has TM dipole and quadrupole modes near the fundamental TM monopole mode used as the $\pi/2$ coupling mode. This situation makes the coupling mode very sensitive to breakdown of the axial symmetry of the annular cavity [2-4]. But, the axial symmetry is inevitably broken by opening the coupling slots. This RF property had prevented the ACS from being put to practical use in linacs.

Increasing the number of coupling slots is expected to reduce the breakdown of axial symmetry. For feasibility studies on multi-slot arrangements, four-slot and eight-slot ACS cold models were made and their RF properties were measured. The following results were obtained [4]:

- With the four-slot arrangement, the axial symmetry can be sufficiently restored to suppress higher order mode mixing with the coupling mode.
- With the eight-slot arrangement, no improvement was found, compared with the four-slot one.

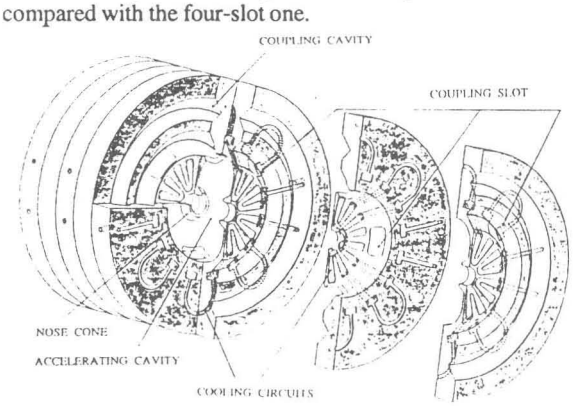

Fig. 1 A cutaway view of a four-slot ACS cavity.

- With the eight-slot arrangement, the total arc length, defined by the arc length of one slot multiplied by the number of slots, increases to attain the same coupling constant as with the four-slot arrangement. Considering the thermal structural properties of the ACS cavity, the four-slot arrangement is a practical solution.

The results of the cold model tests encouraged us to develop high-power models of the four-slot ACS. Three high-β (β=0.78) and one low-β (β=0.52) prototype cavities have been constructed and tested. Results of the RF measurements and high-power tests were reported in References [5, 6].

As an efficient $\pi/2$-mode coupled-cavity structure, the side-coupled structure (SCS) [7] is well known and has been used so far. Its shunt impedance is higher than that of the four-slot ACS by ~5%. Why should we develop the ACS while an efficient SCS linac is already available? The reason is as follows: For future high-brightness linacs, we need an accelerating structure that never deteriorates the beam quality and has a reasonably high shunt impedance.

Distortion of the accelerating field due to the coupling slots becomes a serious problem in high-brightness linacs [8]. Recently, we have found by numerical simulations that the SCS slot configuration tilts the accelerating field in the way that the TM010 mode is mixed with a TE111-like mode [6]. The tilted accelerating field kicks the beam in a transverse direction and may deteriorate the beam quality. On the other hand, the four-slot ACS mixes the accelerating mode with a TE-octupole mode. However, the field strength of the octupole component is negligibly small near the beam axis. Therefore, the four-slot ACS gives an axially symmetric accelerating field to the beam. That motivated us to carry out the R&D work on the four-slot ACS for future high-brightness linacs.

Prototype Cavities

Cavity Design

Table 1 gives design parameters for the low-β and high-β prototype cavities with the staggered slot configuration, where the azimuthal orientation of coupling slot is rotated by 45 degrees from segment to segment. The staggered slot configuration gives a larger coupling factor and a higher shunt impedance than the aligned slot configuration [6].

The shape of the accelerating cell was optimized to give a high shunt impedance, and the coupling cell was designed like a resonant ring of ridged waveguide to reduce the cavity diameter. The cavity parts were machined from oxygen-free copper (OFC) using a super-precision lathe and a milling machine. Four coupling slots were bored at the wall between the accelerating and coupling cells. Before brazing, each cell was tuned to the design frequency within ±100 kHz by fine machining. Finally, the cavity parts were stacked and brazed in a vacuum furnace.

From Table 1, the average power dissipation per accelerating cell amounts to 540 W for the low-β cavity, and 780 W for the high-β one. In order to reduce the thermal detuning, the nosecone region is directly cooled by water circuits in the septum between accelerating cells (see Fig. 1) [9].

TABLE 1
Design and Measured Parameters for the Low-β and High-β Prototype Cavities

frequency	1.296 GHz	
duty factor	3 %	
pulse width	600 μs	
repetition rate	50 Hz	
	low-β prototype	high-β prototype
$\beta = v/c$	0.52	0.78
E_0T	3.0 MV/m	3.5 MV/m
RF peak power	18 kW/cell	26 kW/cell
coupling constant	0.052 measured	0.056 measured
Q	1.5×10^4 / 1.8×10^4	1.9×10^4 / 2.4×10^4
$R(=ZT^2)$ MΩ/m	30 / 37	42 / 54
R/Q Ω/cell	120 / 124	201 / 205
	measured / SuperFish	*measured / SuperFish*

RF Properties

Figure 2 shows a setup for high power test. This setup consists of the low-β cavity (left side) andthe high-β one (right side) coupled via a bridge coupler. The bridge coupler is a 5-cell disk-loaded structure and has an input iris port at the middle cell [10].

Figure 3 shows the electric field distribution on the beam axis for excitation in the $\pi/2$ mode, measured by bead perturbation for the setup in Fig. 2. This field distribution was obtained without retuning the accelerating cells after brazing. For each of the high-β and low-β cavities, the field distribution is uniform within ±0.5% except the end cells, the electric fields of which are higher by ~5%.

Measured RF parameters, Q, $R(=ZT^2)$, R/Q, and coupling constant are also listed in Table 1, together with the theoretical values calculated using SUPERFISH. For the high-β cavity with a coupling constant of 0.056, the shunt impedance is reduced by 22% compared with the theoretical value. This reduction consists of two parts: a reduction of 4% coming from surface imperfections of the cavity wall; the remaining 18% is due to the coupling slots. For the low-β cavity, the coupling constant of which is 0.052, the shunt impedance is reduced by 19%, where 4% is due to the surface imperfections and 15% due to the coupling slots.

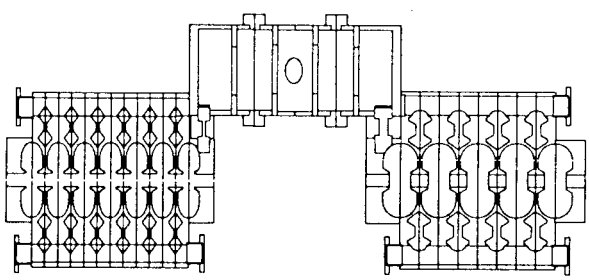

Fig. 2 A schematic drawing of a setup for high power test.

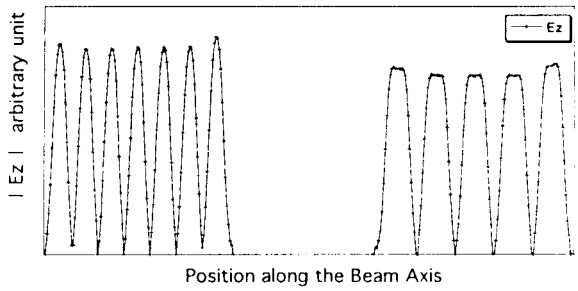

Fig. 3 The electric field distribution on the beam axis for excitation in the $\pi/2$ accelerating mode, measured by bead perturbation for the setup in Fig. 2.

High Power Tests

A series of high-power tests were carried out with a setup as shown in Fig. 2. RF power was supplied by a pulsed klystron of TH2104A by THOMSON-CSF.

The first RF processing was carried out at a low duty factor of 0.1% (100μs × 10Hz). Next, the duty factor was increased step by step up to 2.75% (550μs × 50Hz). Each ACS cavity was evacuated with a 300-l/s turbo-molecular pump, and RF processing was carried out keeping the vacuum pressure level below 2×10^{-6} Torr. The thermal detuning was compensated with three movable tuners installed at the bridge coupler.

At a duty factor of 2.75% (550μs × 50Hz), each of the high-β and low-β prototypes was successfully conditioned up to a peak power level 1.5 times as high as the design value listed in Table 1.

Field Distortion due to Coupling Slots

Numerical simulations using MAFIA were carried out for the SCS and the four-slot ACS in order to study the field distortion caused by the coupling slots. The preliminary results were reported in Ref. [6]. From these simulations, we have found that the SCS slot configuration tilts the accelerating field from the beam axis. An accelerating cell of the SCS has one of the two adjacent coupling cells mounted on the top and the other attached to the bottom, as shown in Fig. 4. This slot configuration is asymmetric with respect to the horizontal plane, and tilts the accelerating field in the way that the TM010 mode is mixed with a TE111-like mode, which is schematically shown in Fig. 4.

Next, we calculated how much the beam is kicked in a transverse direction by the SCS accelerating field mixed with a TE111-like mode when the beam traverses the accelerating gap. Calculations were carried out for two SCS cavities: one is for β=0.52 and the other for β=0.78. Figure 5 shows the ratio of the transverse kick to the longitudinal acceleration, plotted as a function of the coupling constant k. The ratio at $k=0$ is for the axially symmetric single-cell cavity. For example, the SCS of β=0.78 with a coupling constant of 0.05 gives a transverse kick ratio of 8×10^{-3}, which is not negligible.

Comparing the two SCS cases, the transverse kick by the SCS of β=0.78 is more than five times as large as that by the SCS of β =0.52. This can be well explained as follows: The TE111 frequency depends on the cell length, and becomes lower as the cell becomes longer. The TE111-mode mixing increases as its frequency comes down from 3.3 GHz for β=0.52 to 2.3 GHz for β=0.78 toward the accelerating-mode frequency 1.3 GHz.

Fortunately, the direction of the transverse kick by the tilted accelerating field is reversed from gap to gap in an SCS linac. Therefore, the transverse kicks by two adjacent gaps cancel out. However, this counterbalance is assured only when there are no errors in the field amplitude or phase.

For the four-slot configuration of the ACS, it was found that the accelerating field is mixed with a TE-octupole mode. However, the field strength of the octupole component is negligibly small near the beam axis. Therefore, the four-slot ACS gives a distortion-free accelerating field to the beam. Figure 5 shows that the transverse kick ratio of the ACS with $k = 0.05$ is almost equal to zero.

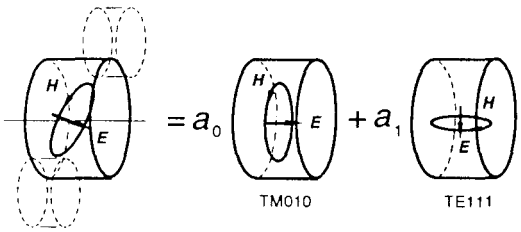

Fig. 4 A schematic drawing showing how the SCS slot configuration tilts the accelerating field.

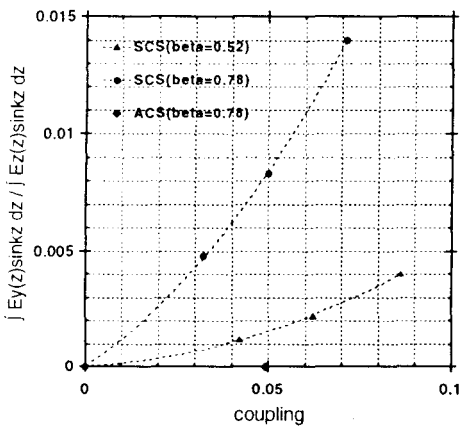

Fig. 5 For two SCS cases with different βs, the ratio of the transverse kick to the longitudinal acceleration is plotted as a function of the coupling constant, compared with that for a four-slot ACS.

R&D work on production models

After the success in the prototype cavities, subsequent R&D work on production models has started. Machining and brazing processes applied to the prototype cavities were re-examined for cavity production.

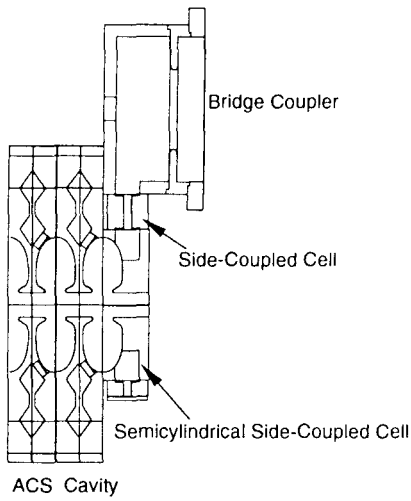

Fig. 6 A semicylindrical side-coupled cell is attached to the end cell to counterbalance the side-coupled cell between the ACS cavity and the bridge coupler.

The construction of an 18-cell ACS cavity at β=0.504 is underway. This cavity has a semicylindrical side-coupled cell attached to the end cell as shown in Fig. 6. This is to counterbalance the side-coupled cell between the ACS cavity and the bridge coupler.

The four-slot ACS, which has a distortion-free accelerating field and a reasonably high shunt impedance, is promising for future high-brightness linacs.

References

[1] V.G. Andreev et al., "Study of High-Energy Proton Linac Structures", Proc. 1972 Proton Linac Conf., pp. 114-118, 1972.
[2] R.A. Hoffswell and R.M. Laszewski, "Higher Modes in the Coupling Cells of Coaxial and Annular-Ring Coupled Linac Structure", IEEE Trans. on Nucl. Sci., Vol. 30, pp. 3588-3589, 1983.
[3] R.K. Cooper et al., "Radio-Frequency Structure Development for the Los Alamos/NBS Racetrack Microtron", Preprint LA-UR-83-95, 1983.
[4] T. Kageyama et al., "A New Annular Coupled Structure Suppressing Higher Order Modes' Mixing with the π/2 Coupling Mode", Part. Accel., Vol. 32, pp. 33-38, 1990.
[5] T. Kageyama et al., "A High-Power Model of the ACS Cavity", Proc. 1990 Linac Conf., Albuquerque, USA, LA-12004-C, pp. 150-152, 1990.
[6] T. Kageyama et al., "Development of Annular Coupled Structure", Proc. 1992 Linac Conf., Ottawa, Ontario, Canada, AECL-10728, Vol. 2, pp. 456-458, 1992.
[7] E.A. Knapp, B.C. Knapp, and J.M. Potter, Rev. Sci. Instr., Vol. 39, pp. 979-991, 1968.
[8] R.L. Sheffield et al., "Physics Design of the High Brightness Linac for the Advanced Free-Electron Laser Initiative at Los Alamos", Nucl. Instr. and Meth., Vol. A318, pp. 282-289, 1992.
[9] K. Yoshino et al., "Studies on Water-Cooling of an ACS High-Power Model" (in Japanese), Proc. 1991 Linac Meeting in Japan, Tokyo, pp. 242-244, 1991.
[10] Y. Morozumi et al., "Multi-Cavity Bridge Coupler", Proc. 1990 Linac Conf., Albuquerque, USA, LA-12004-C, pp. 153-155, 1990.